

A numerical study of non-Newtonian blood flow in stenosed coronary artery bypass with grafts

D. Poltem* B. Wiwatanapataphee* Y. H. Wu†
Y. Lenbury*

(Received 28 October 2005; revised 18 August 2006)

Abstract

We investigate the behaviour of the pulsatile blood flow in a stenosed right coronary artery with a bypass graft. The human blood is assumed as a non-Newtonian fluid and its viscous behaviour is described by the Carreau model. The transient phenomena of blood flow through the stenosed region and the bypass graft are simulated for five cardiac cycles by solving the three dimensional unsteady Navier–Stokes equations coupled with the non-Newtonian model. Effects of the time variations of pulsatile velocity and pulse pressure are taken

*Dept. of Mathematics, Faculty of Science, Mahidol University, Bangkok, THAILAND.
<mailto:scbw@mahidol.ac.th>

†Dept. of Mathematics and Statistics, Curtin Univ. of Tech., WESTERN AUSTRALIA.
<mailto:yhwu@maths.curtin.edu.au>

See <http://anziamj.austms.org.au/V47EMAC2005/Poltem> for this article, © Austral. Mathematical Soc. 2006. Published October 2, 2006. ISSN 1446-8735

into account. The influence of the bypass angle on the flow interaction between the jet flow from the native artery and the flow from the bypass graft is investigated. Distributions of velocity, pressure and wall shear stresses are determined under various conditions. The results show that the blood pressure in the stenosed artery drops dramatically in the stenosis area and that high wall shear stresses occur around the stenosis site.

Contents

1 Introduction	C278
2 The underlying boundary value problem	C280
3 A numerical algorithm based on the finite element method	C282
4 Numerical results	C284
5 Conclusions	C289
References	C290

1 Introduction

Atherosclerosis lesion or plaque is a common form of cardiovascular diseases. Plaque development consists of three stages which are the initial stage in which the intimal thickening starts, the growth stage, and the final stage in which the plaque becomes severe enough to affect the blood supply to the heart muscle. Occlusion of arteries due to the atherosclerotic plaque formation is the leading cause of mortality in developed countries [4]. In recent years, surgical treatments of cardiovascular diseases has developed

rapidly, and coronary artery bypass grafting (CABG) has been widely used for patients with severe coronary artery diseases. The bypass graft technique has been used worldwide for many years. However, up to 25% of the grafts become occluded in one year and up to 50% occluded in ten years [9]. Intimal hyperplasia which is related to the distribution of wall shear stress (WSS) is an important factor related to the failure of the coronary bypass surgery. The features of the wall shear stress and the wall shear rate are associated with the development of the intimal hyperplasia on the native artery bed. In general, atherosclerotic lesions in the coronary arteries are related to low and oscillating wall shear stress [12]. Once the magnitude of the wall shear stress reaches a value higher than 400 dyn/cm^2 , the endothelium surface is irreversibly damaged [8]. Atherosclerotic lesions are also related to the high shear rate. Previous investigations led to better understanding of the flow, which helps to disclose the reason of atherogenesis development.

The flow in the coronary artery with a bypass graft was studied by numerous authors [2, 3, 10]. In these studies, blood was modeled as a Newtonian fluid. The viscoelasticity of blood was ignored under the assumption that the shear rate is larger than 100 s^{-1} . In the last two decades, many researchers [1, 7, 6] numerically investigated the influence of the non-Newtonian properties of blood on the flow in three-dimensional coronary artery models. All of the above studies investigated blood flow based on some assumptions, for instance, constant velocity at the inlet and constant pressure at the outlet. Until recently, none of the studies concentrated on the influence of the bypass graft angle using a non-Newtonian model on the flow patterns and the wall shear stresses in the artery.

In this study, we simulate the unsteady non-Newtonian blood flow in the 75% stenosed right coronary artery. The three-dimensional Navier–Stokes equations coupled with a non-Newtonian model are solved numerically using the Galerkin finite element method. Effect of using different bypass graft angles, which are 45° , 60° and 90° , on the flow pattern is investigated.

2 The underlying boundary value problem

Human blood is modeled as an incompressible non-Newtonian fluid and its flow in the artery bypasses is assumed to be laminar. The governing equations consist of the continuity equation and the Navier–Stokes equations:

$$\nabla \cdot \mathbf{u} = 0, \quad (1)$$

$$\frac{\partial \mathbf{u}}{\partial t} + \mathbf{u} \cdot \nabla \mathbf{u} = \frac{1}{\rho} \nabla \cdot \boldsymbol{\sigma}, \quad (2)$$

where \mathbf{u} denotes the blood velocity vector, ρ is the density of blood, $\boldsymbol{\sigma}$ is the total stress tensor which is related to the pressure p and shear stress $\boldsymbol{\tau}$ by $\boldsymbol{\sigma} = -p\mathbf{I} + \boldsymbol{\tau}$, the shear stress tensor depends on the rate of deformation tensor \mathbf{D} by $\boldsymbol{\tau} = 2\eta(\dot{\gamma})\mathbf{D}$, where $\mathbf{D} = \frac{1}{2}(\nabla \mathbf{u} + \nabla \mathbf{u}^T)$, η and $\dot{\gamma}$ denote the viscosity of blood and shear rate, respectively. The viscosity of blood η has been found to depend on the shear rate $\dot{\gamma}$, and various models have been proposed to describe the relation between η and $\dot{\gamma}$. In this work, we use Carreau's shear thinning model, namely

$$\eta = \eta_\infty + (\eta_0 - \eta_\infty) [1 + (\lambda\dot{\gamma})^2]^{(n-1)/2}, \quad (3)$$

where $\dot{\gamma} = \sqrt{2 \operatorname{tr}(\mathbf{D}^2)}$ is a scalar measure of the rate of deformation tensor, η_0 and η_∞ denote the zero shear viscosity and the infinite shear viscosity. The consistency index, n , is a parameter between 0 and 1. Based on Cho and Kensey [5], the parameters have the typical values $\eta_\infty = 0.0345 \text{ g cm}^{-1} \text{ s}^{-1}$, $\eta_0 = 0.56 \text{ g cm}^{-1} \text{ s}^{-1}$, $n = 0.3568$ and $\lambda = 3.313 \text{ s}$.

To completely define the flow problem, boundary conditions for the velocity and pressure fields must be specified. For a typical coronary artery bypass grafting system, the boundary of the computation region consists of four parts, namely the inflow surface of the native artery and the bypass graft, the artery wall, and the outflow boundary.

On the inflow surfaces, the velocity is set to the pulsatile velocity $\bar{u}_{\text{in}}(t) = Q(t)/A$ where A is the cross section area of the inlet surface [cm^2] and $Q(t)$ is

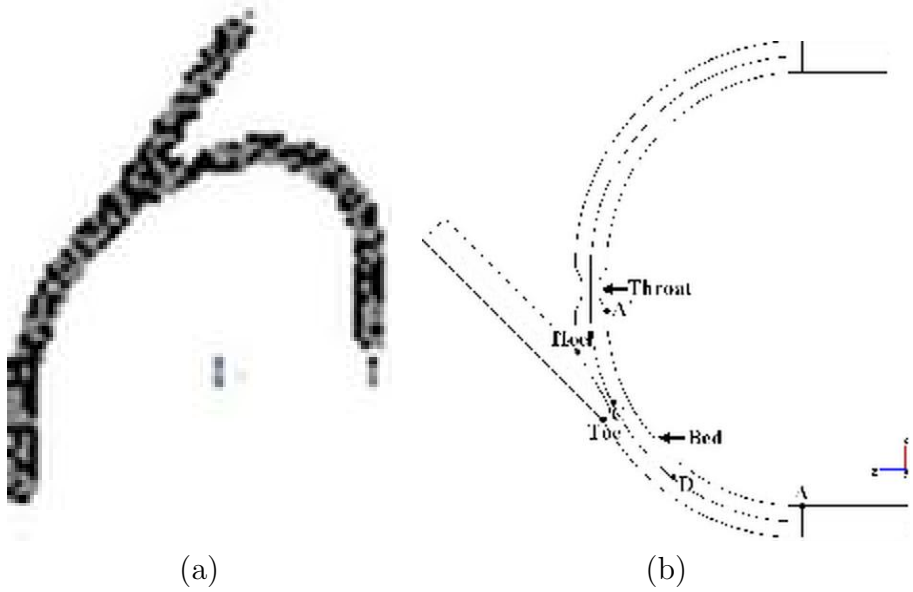


FIGURE 1: Geometry of the three-dimensional model for a 75% stenosed right coronary artery with a bypass graft: (a) global view; (b) $x-z$ view.

the pulsatile flow rate [ml/s] [2]. The flow waveform is written in the form of the following Fourier series:

$$Q(t) = \bar{Q} + \sum_{n=1}^5 Q_n \cos(n\omega t - \alpha_n), \quad (4)$$

where \bar{Q} is the mean volume flow rate. The no-slip condition is applied to the artery wall. On the outflow boundary, the normal stress is specified:

$$\boldsymbol{\sigma} \cdot \mathbf{n} = -p(t)\mathbf{n},$$

where \mathbf{n} is the unit normal vector to the outlet section. We assume the pressure at the outlet to be the pulse pressure, which in the form of a Fourier series is

$$p(t) = \bar{p} + \sum_{n=1}^5 p_n \cos(n\omega t - \beta_n), \quad (5)$$

where \bar{p} is the mean pressure, $\omega = 2\pi/T$ is the angular frequency with period $T = 0.75$ s.

In summary, the fluid flow in the coronary artery bypass graft is governed by the following boundary value problem.

BVP: Find \mathbf{u} and p such that the field equations (1) and (2) are satisfied in Ω and all boundary conditions are satisfied.

3 A numerical algorithm based on the finite element method

The variational statement corresponding to the BVP is VBVP: Find \mathbf{u} and p in $H^1(\Omega)$ such that for all \mathbf{w}^u and w^p in $H_0^1(\Omega)$, all boundary conditions are satisfied and

$$(\nabla \cdot \mathbf{u}, w^p) = 0,$$

$$\left(\frac{\partial \mathbf{u}}{\partial t}, \mathbf{w}^u \right) + (\mathbf{u} \cdot \nabla \mathbf{u}, \mathbf{w}^u) = \frac{1}{\rho} (\nabla \cdot [-pI + \eta(\nabla \mathbf{u} + (\nabla \mathbf{u})^T)], \mathbf{w}^u), \quad (6)$$

where (\cdot, \cdot) denotes the inner product on the square integrable function space $L^2(\Omega)$, $H^1(\Omega)$ is the Sobolev space $W^{1,2}(\Omega)$ with norm $\|\cdot\|_{1,2,\Omega}$ and $H_0^1(\Omega) = \{v \in H^1(\Omega) \mid v = 0 \text{ on the Dirichlet boundary}\}$. Standard procedures for the development of the Galerkin finite element formulation lead to the following system

$$\begin{aligned} C^T U &= 0, \\ M\dot{U} + A(U)U + \bar{C}P &= 0. \end{aligned} \quad (7)$$

Using the backward Euler differentiation scheme for a typical time step, $t_n \mapsto t_{n+1}$, we have

$$\begin{aligned} C^T U_{n+1} &= 0, \\ \left(\frac{M}{\Delta t_n} + A \right) U_{n+1} + \bar{C}P_{n+1} &= \frac{M}{\Delta t_n} U_n, \end{aligned} \quad (8)$$

which is nonlinear because A depends on U_{n+1} . To deal with this nonlinearity for an iterative solution of (8), we use the following iterative updating

$$\begin{aligned} C^T U_{n+1}^{i+1} &= 0, \\ \left(\frac{M}{\Delta t_n} + A_{n+1}^i \right) U_{n+1}^{i+1} + \bar{C}P_{n+1}^{i+1} &= \frac{M}{\Delta t_n} U_n^i, \end{aligned} \quad (9)$$

where the superscript i denotes evaluation at the i th iteration step. Therefore, in a typical time step, $t_n \mapsto t_{n+1}$, starting with $U_{n+1}^0 = U_n$, we determine U_{n+1}^{i+1} and P_{n+1}^{i+1} through solving the system (9) repeatedly until $\|U_{n+1}^{i+1} - U_{n+1}^i\| < \varepsilon_u$ and $\|P_{n+1}^{i+1} - P_{n+1}^i\| < \varepsilon_p$.

By repeatedly using the above procedure for $n = 0, 1, 2, \dots$ we determine the state U and P of the system at t_0, t_1, t_2, \dots . If the norm $\|U_{n+1} - U_n\|$ and $\|P_{n+1} - P_n\|$ are sufficiently small, then the solution approximates the steady state.

4 Numerical results

Flow simulations were conducted under a typical physiological condition. The fluid properties are typical of human blood with a density 1.06 g cm^{-3} [11]. The computation region, as shown in Figure 1, represents the right coronary artery with a 75% stenosis located 3.95 cm from the inlet boundary. The diameter of the native artery is $D = 0.3 \text{ cm}$, and the diameter of the graft is 0.288 cm. The length of the artery in this investigation is 8.5 cm.

We simulate the three-dimensional blood flow through the stenosed right coronary artery with the 45° , 60° and 90° bypass operations. The mesh as shown in Figure 1 consists of 15819 tetrahedral elements with 27030 nodes and 85068 degrees of freedom. To simulate the flow patterns in successive cycles, each cycle is divided into 1051 time steps with step size 3.57 ms.

Figure 2 shows the velocity profile of blood flow in the right coronary artery with the 45° bypass graft. It clearly outlines how the flow goes through the stenosed artery. The velocity at the stenosis region suddenly tends to decrease at the downstream when we use the bypass operation. Compared with the results obtained from the model without bypass grafts, the blood speed tends to decrease in the model with the bypass graft. The results also indicate that the residual flow from the stenosed artery creates a jet flow interacting with the flow from the graft. When it flows to the heel, it hits the flow from the graft. This reduces blood speed near the graft region. The relationship between the pressure and the velocity is explained in Figures 3 and 4. The figures shows the pressure distribution along the arterial axis and the velocity distribution along the radial axis at the throat during the systolic period. They depict that the pressure drops very fast around the stenosis site for any bypass graft angles, and produces high blood speed in this region. In the model without bypass operation, the velocity in the far distal part is very low compared to the one with the bypass operation. In the model without bypass graft, the maximum blood speed in the far distal part is 40.41 cm/s. However, when we use the 45° , 60° and 90° angles

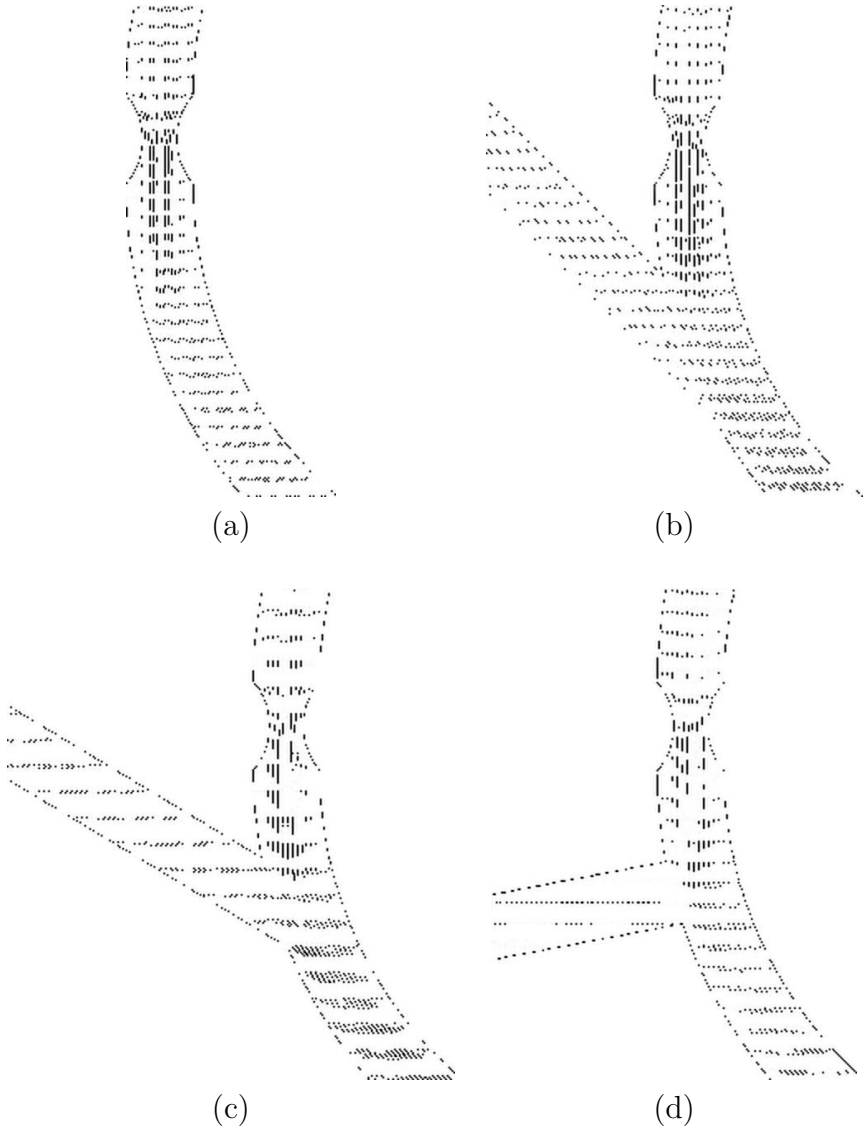
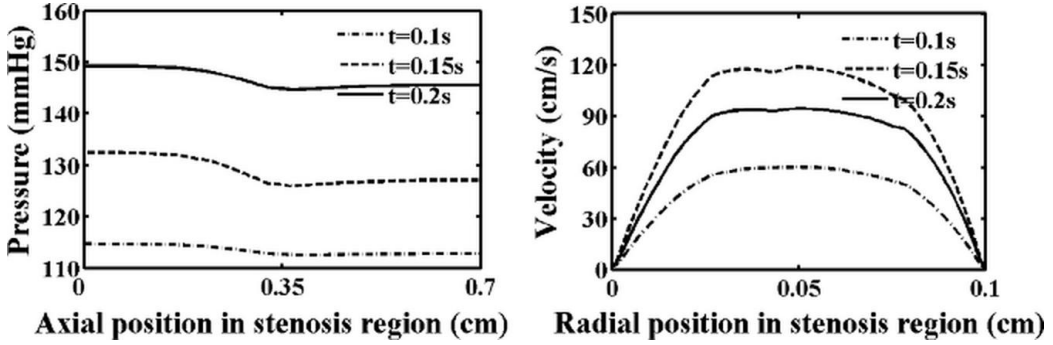
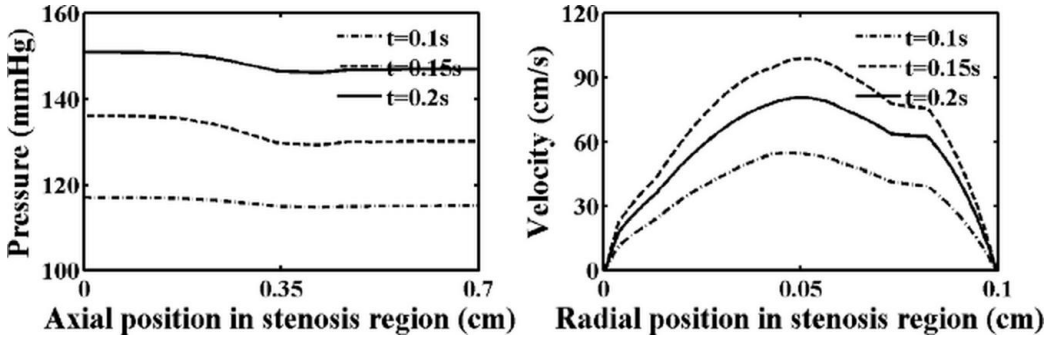


FIGURE 2: The velocity profiles of blood flow in the right coronary artery on the xz plane at the instant of time $t = 0.1\text{s}$ (beginning of the systole): (a) with no bypass, and (b)–(d) with bypass operation 45° , 60° , and 90° , respectively.

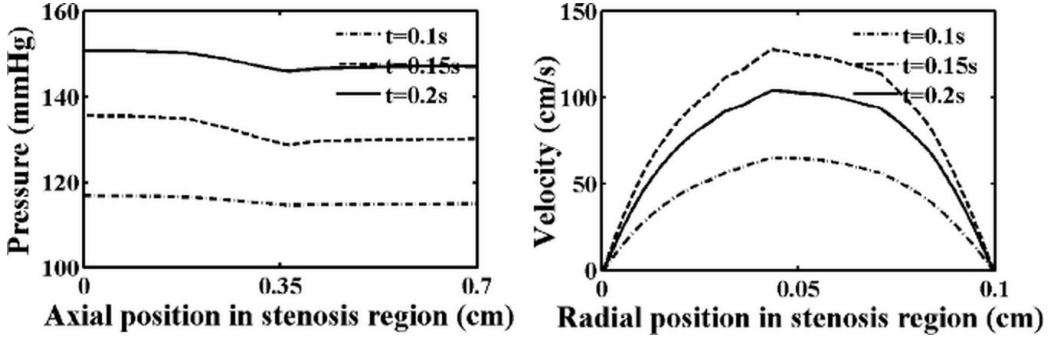


(a)

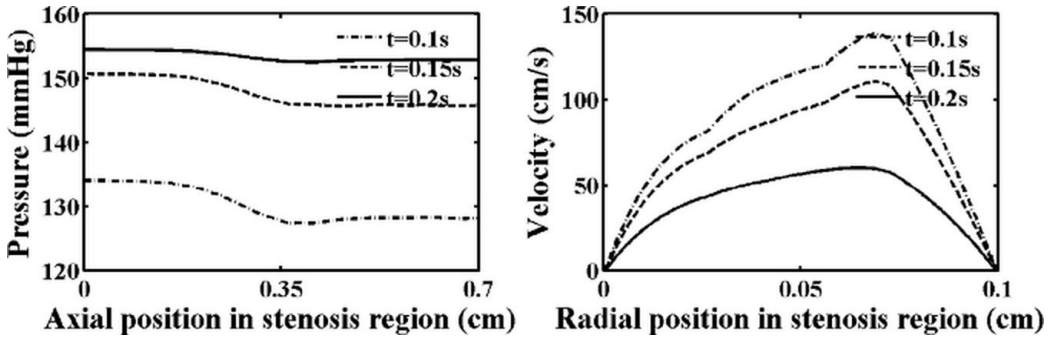


(b)

FIGURE 3: the distributions of pressure and velocity in the stenosis region at the systole period: (a) without bypass graft, (b) with bypass graft angles 45° .



(c)



(d)

FIGURE 4: the distributions of pressure and velocity in the stenosis region at the systole period: (c)–(d) with bypass graft angles 60° and 90° , respectively.

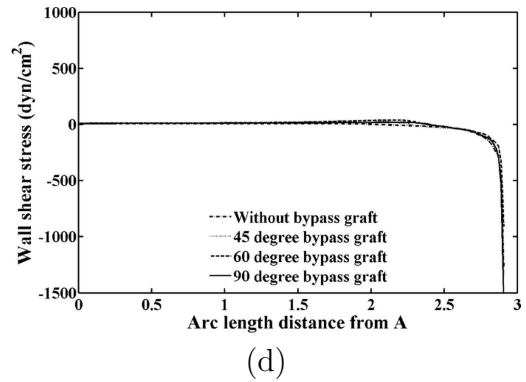
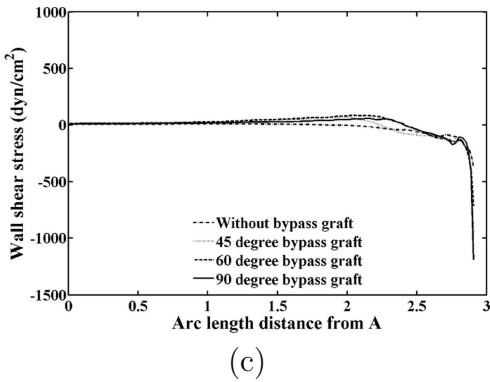
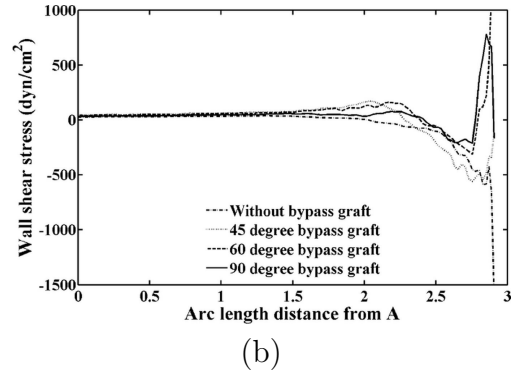
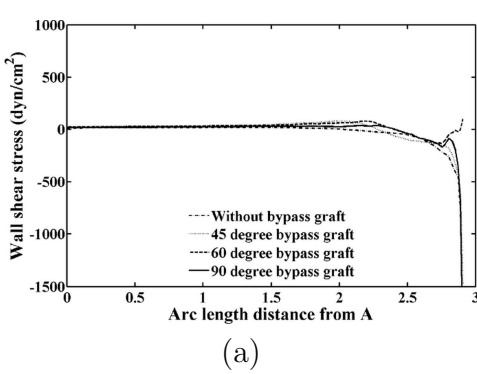


FIGURE 5: The distribution of the wall shear stress along the bed of artery, (along the line from A to A', see Figure 1(b)), at various times: (a) $t = 0.15$ s, (b) $t = 0.25$ s, (c) $t = 0.35$ s and (d) $t = 0.5$ s.

of bypass graft, the blood speed in the far distal part tends to increase and reaches 78.08, 70.91 and 54.07 cm / s, respectively. In addition, the maximum blood speed in the far distal part decreases as the angle of bypass graft increases. To determine the critical flow condition, prediction of the wall shear stress is essential. Thus we plot the wall shear stress along the bed of the host artery in Figure 5 to show the influence of bypass graft. The results indicate that the magnitude of wall shear stress varies between 0 and 4150 dyn / cm² and high negative wall shear stress occurs around the stenosis site.

5 Conclusions

This study provides a better understanding of the bypass graft effects on blood flow through a 75% stenosed right coronary artery. The work is based on the use of a non-Newtonian model and the Bubnov–Galerkin finite element method. The use of the pulsatile velocity at the inlet and the pulse pressure at the outlet enables one to simulate the transient behaviour of blood flow in the artery. Comparing the results for different angles of bypass grafts, the one with a 45° graft angle seems to perform better. The results show that the wall shear stress is low in the bed of the stenosed artery but there exist negative shear stresses in the stenosis region, which may lead to the development of atherosclerotic lesions. In addition to the effect on flow pattern, there may have other ways which affect the formation of atherosclerosis. The proper choice of the diameter of the graft might improve the balance of inflow and outflow in the coronary artery. To improve the accuracy of results, the effect of porous wall and wall deformation must be included; further research work will be carried out to include the effect of wall deformation.

Acknowledgements: The project is supported by the Commission on Higher Education Staff Development Project Scholarship, the Thailand Research Fund and the 2005 Australia Endeavour Chueng Kong Awards. The

authors also thank the Division of Cardiac Surgery, Heart Institute Saint Louis Hospital and Foundation for providing some data for the analysis.

References

- [1] M. J. Barbara, R. J. Peter, C. Stuart, K. David, Non-Newtonian blood flow in human right coronary arteries: steady state simulations, *J. Biomech*, **37**, 2004, 709–720. [C279](#)
- [2] C. Bertolotti, V. Deplano, J. Fuseri, P. Dupouy, Numerical and experimental models of post-operative realistic flows in stenosed coronary bypasses, *J. Biomech*, **34**, 2001, 1049–1064. [C279](#), [C282](#)
- [3] M. Bonert, J. G. Myers, S. Fremes, J. Williams, C. R. Ethier, A numerical study of blood flow in coronary artery bypass graft side-to-side anastomoses, *Annals of Biomedical Engineering*, **30**, 2002, 599–611. [C279](#)
- [4] C.G. Caro, J.M. Fitz-Gerald, R.C. Scliroter, Atheroma and arterial wall shear: observation, correlation and proposal of a shear dependent mass transfer mechanism for atherogenesis, *Proc. Roy. Soc. B*, **177**, 1971, 109–159. [C278](#)
- [5] Y. I. Cho, K. R. Kensey, Effects of the non-Newtonian viscosity of blood on flows in a diseased arterial vessel. Part 1: steady flows, *Biorheology*, **28**, 1991, 241–262. [C280](#)
- [6] J. Hun, W. C. Jong, G. P. Chan Asymmetric flows of non-Newtonian fluids in symmetric stenosed artery, *Korea–Australia Rheology Journal*, **16**, 2004, 101–108. [C279](#)
- [7] C. Jie, L. Xi-Yun, Numerical investigation of non-Newtonian blood flow in a bifurcation model with a non-planar branch, *J. Biomech*, **37**, 2004, 1899–1911. [C279](#)

- [8] D. N. Ku, Blood flow in arteries, *Annu Rev. Fluid Mech.*, **29**, 1997, 399–434. C279
- [9] Y. Papaharilaou, D. J. Doorly, S. J. Sherwin, The influence of out-of-plane geometry on pulsatile flow within a distal end-to-side anastomosis, *J. Biomech*, **35**, 2002, 1255–1239. C279
- [10] M-H. Song, M. Sato, Y. Ueda, Three-dimensional simulation of coronary artery bypass grafting with the use of computational fluid dynamics, *Surg. Today*, **30**, 2000, 993–998. C279
- [11] D. Tang, C. Yang, S. Kobayashi, Ku D. N., Steady flow and wall compression in stenotic arteries: a three-dimensional thick-wall model with fluid-wall interactions, *J. Biomech Eng*, **123**, 2001, 548–557. C284
- [12] E. S. Weydahl, J. M. Moore Jr., Dynamic curvature strongly affects wall shear rates in a coronary artery bifurcation model, *J. Biomech*, **34**, 2001, 1189–1196. C279